AD-A162 772 INVESTIGATIONS INTO THE ORIGINS OF THE PHYSICAL STRUCTURE OF THIN FILMS(U) PENNSYLVANIA STATE UNIV UNIVERSITY PARK MATERIALS RESEARCH LAB R MESSIER

1/1

UNCLASSIFIED 25 OCT 85 AFOSR-TR-85-1105 AFOSR-84-0149 F/G 7/4 NL

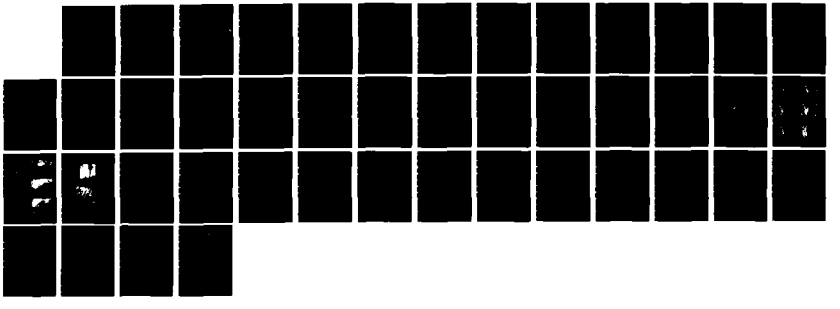

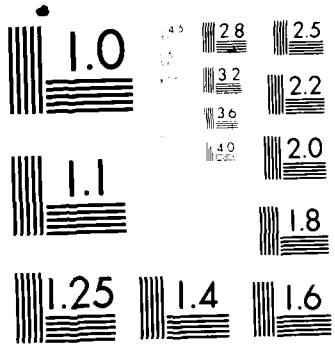

UNCLASSIFIED

RITY CLASSIFICATION OF THIS PAGE

AD-A162 772

REPORT DOCUMENTATION PAGE

EPORT SECURITY CLASSIFICATION: UNCLASSIFIED	1b. RESTRICTIVE MARKINGS
CURITY CLASSIFICATION AUTHORITY	3. DISTRIBUTION/AVAILABILITY OF REPORT: The United States Governemnt is authorized to reproduce and distribute this report for government purposes.
CLASSIFICATION/DOWNGRADING SCHEDULE	
FORMING ORGANIZATION REPORT NUMBER(S)	5. MONITORING ORGANIZATION REPORT NUMBER(S): AFOSR-84-0149
ME OF PERFORMING ORGANIZATION: The Pennsylvania State University; 6b. OFFICE SYMBOL (If applicable)	7a. NAME OF MONITORING ORGANIZATION: AFOSR/NE
6c. ADDRESS (City, State and ZIP Code): Materials Research Laboratory, University Park, PA 16802	7b. ADDRESS (City, State and ZIP Code): Same as 6c
8a. NAME OF FUNDING/SPONSORING ORGANIZATION: Air Force Office of Scientific Research; 8b. OFFICE SYMBOL (If applicable): NE	9. PROCUREMENT INSTRUMENT IDENTIFICATION NUMBER: AFOSR-84-0149
8c. ADDRESS (City, State and ZIP Code): Bolling Air Force Base, DC 20332	10. SOURCE OF FUNDING NOS.

PROGRAM ELEMENT NO.	PROJECT NO.	TASK NO.	WORK UNIT NO.
61102F	2306	B2	

11. TITLE (Include Security Classification): Investigations into the Origins of the Physical Structure of Thin Films

12. PERSONAL AUTHOR(S): Russell Messier

13a. TYPE OF REPORT	13b. TIME COVERED	14. DATE OF REPORT (Yr., Mo., Day)	15. PAGE COUNT
ANNUAL TECHNICAL	FROM 7/01/84 TO 6/30/85	1985 October 25	9

16. SUPPLEMENTARY NOTATION

17. COSATI CODES			18. SUBJECT TERMS (Continue on reverse if necessary and identify by block number)
FIELD	GROUP	SUB. GR.	
			Thin Films, Sputtering, Ion-Assisted Deposition, Morphology, Random Aggregation, Fractals, Morphology Evolution

19. ABSTRACT (Continue on reverse if necessary and identify by block number)

The random ballistic aggregation of atoms onto a surface under low adatom mobitity conditions leads to clustering and evolution of growth cones from these random clusters. The connections between these basic physical processes and the resulting wide variety of thin film morphologies (both top surface and cross-section) are being made in an attempt to quantify morphology, and ultimately properties. The research can be divided into four research thrust areas: 1.) controlled film preparation; 2.) morphological characterization of the resulting films; 3.) image enhancement/quantification of micrographs of morphology; and 4.) conceptual and computer modeling of the morphology. This report describes our progress in each of these areas.

DTIC FILE COPY

20. DISTRIBUTION/AVAILABILITY OF ABSTRACT	21. ABSTRACT SECURITY CLASSIFICATION
UNCLASSIFIED/UNLIMITED ☑ SAME AS RPT. ☐ DTIC USERS ☐	UNCLASSIFIED

22a. NAME OF RESPONSIBLE INDIVIDUAL	22b. TELEPHONE NUMBER (Include Area Code)	22c. OFFICE SYMBOL
Capt Kevin Malloy	202-767-4931	NE

DD FORM 1473, 83 APR EDITION OF 1 JAN 73 IS OBSOLETE.

SECURITY CLASSIFICATION OF THIS PAGE

ANNUAL TECHNICAL REPORT

to

Air Force Office of Scientific Research
Bolling Air Force Base, DC 20332

on

Investigations into the Origins of the Physical Structure of Thin Films

Grant No. AFOSR-84-0149

for period

July 1, 1984 to June 30, 1985

Submitted by

Russell Messier
Materials Research Laboratory and
Department of Engineering Science and Mechanics
The Pennsylvania State University
University Park, PA 16802

Abstract

The random ballistic aggregation of atoms onto a surface under low adatom mobility conditions leads to clustering and evolution of growth cones from these random clusters. The connections between these basic physical processes and the resulting wide variety of thin film morphologies (both top surface and cross-section) are being made in an attempt to quantify morphology, and ultimately properties. The research can be divided into four research thrust areas: 1.) controlled film preparation; 2.) morphological characterization of the resulting films; 3.) image enhancement/quantification of micrographs of morphology; and 4.) conceptual and computer modeling of the morphology. This report describes our progress in each of these areas.

INTRODUCTION

The overall objective of this research grant is to establish a quantitative description of the morphology of thin films which results from the random aggregation of atoms onto a surface. It is a supposition of this work that a quantitative description and understanding of thin film properties is not possible until a detailed and quantitative model of morphology is established. The paths for achieving this objective are manifold and much of the work during this first year was involved in initiating a number of separate but related research thrusts. Each of these research areas will be briefly described in this report, as will their eventual connections during the second and third years.

The thin film morphology which is the focus of this grant is that which occurs from the random aggregation of vapor species onto a surface such that the species have low mobility. Specifically, this occurs for most, if not all, inorganic materials deposited at $T/T_m \lesssim 0.5$, where T = substrate surface temperature and T_m = the material melting point, both in °K. The morphology typically seen has been described as cauliflower-like or honeycomb-like when observed at the top surface and columnar or fibrous when viewed in cross-section. As indicated by these terms, the description is qualitative and relies mainly on human perception of ordering in an ill-defined, almost random structure. Furthermore, concurrent ion bombardment of the growing film during otherwise low adatom mobility deposition generally leads to denser and smoother top surface morphologies. The exact mechanisms and ways in which morphology is altered during ion-assisted deposition are not understood.

There are four general research thrusts: 1.) controlled film preparation; 2.) morphological characterization of resulting films; 3.) image enhancement/quantification of micrographs of morphology; and 4.) conceptual and computer modeling of the morphology.

Thin Film Preparation

For the preparation of thin films under controlled conditions, a deposition system was designed, constructed and just became operational. It is a turbo-molecular pumed system with a quadrupole mass spectrometer and automatic gas flow control system for controlled reactive sputtering experiments. The magnetron sputtering source is being specially designed with an enclosing shroud so that the gas for the plasma will flow in the vicinity of the sputtering target surface mainly and then be directly pumped. This will prevent the sputtering gases from interfering significantly with the substrate surface and the ion gun, which will be added during the second year. Thus reactive gases can be added directly at the substrate or indirectly through the ion gun. This system will allow us to prepare films with controlled: temperature; bombardment species, energy and flux; angle of deposition and ion bombardment; and ion-surface reactions.

Thin Film Morphology

During this first year experiments were carried out in a conventional rf-sputtering system in order to prepare films with controlled density. Specifically amorphous Ge films were prepared and characterized by microscopy and spectroscopic ellipsometry in order to obtain a correlation between morphology and film density (and indirectly voids, i.e., low density regions). Amorphous Ge has been studied extensively in the past and because of its relatively high atomic weight, gives good contrast in microscopy. In addition, it has been found by spectroscopic ellipsometry that the highest density films are 8% greater than crystalline density, a result of practical and theoretical significance [J.R. Blanco, R. Messier, K. Vedam, and P.J. McMarr, 'Spectroscopic Ellipsometry Study of rf-sputtered a-Ge Film,' Mat.

Res. Soc. Symp. Proc. 38, 301 (1985)]. However, since this absolute density is based upon an experimental result which has been generally accepted in the literature for over ten years [G.A.N. Connell, R.J. Temkin, and W. Paul, Adv. Phys. 22, 643 (1973)] but not rigorously tested, we are carrying out in this study our own independent measurements of absolute density - a non-trivial task for thin films - using a combination of Rutherford backscattering (with Sandia Labs), nuclear activation and precise film thickness (with NBS) measurements.

An important suggestion of this study is that the densest films are achieved when a high energy bombardment process ($\gtrsim$200eV) is present. With the new deposition system we will be able to prepare films under systemmatically varied bombardment energies and to test this suggestion. Also the information gained in this study of a-Ge should be direct applicable to a-Si. The changes in density with ion bombardment will be essential before we can determine a more complete model which might include voids and internal oxide along void boundaries in addition to the density of un-voided material. Such multi-phase, quantitative modeling of thin layer materials by spectroscopic ellipsometry is possible [K. Vedam, P.J. McMarr, and J. Narayan, 'Nondestructive Depth Profiling by Spectroscopic Ellipsometry,' Appl. Phys. Lett. 47, 339 (1985)] and will be applied to our vapor-deposited films in cooperation with Professor K. Vedam.

Pyrolytic graphite films prepared by the thermal decomposition of methane and hydrogen make an interesting system for study since they can be prepared very thick (5cm) and can be cleaved easily into 1mm thick slabs. This allowed for the systemmatic evolution series of morphology development as well as a magnification series at a fixed level of morphology development. These and related studies on the evolution of morphology form the basis for our suggestions that the internal boundaries in thin films prepared under low

mobility conditions are analogous to a random Sierpinski gasket and are fractal. A preprint of this paper is included in this report.

Image Enhancement/Quantification of Morphology

The top surface morphology has been described as cauliflower-like or honeycomb-like which indicates a cellular-type of structure. What is needed is a quantification of the size, shape, and distribution of these 'cells'. Unfortunately, the cellular nature is rather ill-defined and thus it will be necessary to enhance these features so as to form closure which our perception tells us is realistic. During this year we have worked in collaboration with Dr. Alain Mocellin (Ecole Polytechnique Federal in Lusanne, Switzerland) and Dr. G.G. Wu (Nankai University in Tianjin, Peoples Republic of China) using image analysis and false color photography techniques, respectively. In addition, we have worked with Dr. J. Lebiezik (Lemont Scientific in State College, PA) in exploring techniques for image enhancement and extracting information about the surface roughness relief measurements. Because of the experience gained, along with the fact that the Materials Research Laboratory just recently purchased a Lemont OASYS image analysis system, we expect to make significant progress within the next year. Furthermore, the OASYS system is directly coupled with our high resolution SEM (ISI Model DS-130) so that real-time insitu image enhancement of our micrographs will be possible. Future plans include interfacing the OASYS system with our high resolution analytical electron microscope (Philips Model 420) and fast fourier transform analysis of the images in real-time.

The Fourier transform analysis of various graphite morphologies have been performed as part of a Bachelor of Engineering thesis (see publications list). The digitization and grey-level scheme for recording the images was relatively low resolution and the methods for data analysis cumbersome and slow. Again,

with the new OASYS system we expect better and faster results. A conclusion from this study is that the thin film morphologies showed self-similarity as indicated by their similar Fourier transforms. These random fractal morphologies were also compared to geometeric fractals at various stages of evolution (Koch snowflakes and Sierpinski gaskets) which also displayed a similarity in their Fourier transforms.

Conceptual and Computer Modeling of Morphology

The fractal model we have proposed for describing the internal boundaries comprising thin film morphology still needs to be rigorously tested both experimentally and theoretically. Such testing provides a conceptual framework within which we are designing and carrying out our experiments. Semi-quantitative experimental results obtained to date in the current program and a related but separately funded NSF contract [and summarized in two recently completed Ph.D. theses: A.P. Giri (1984) 'Non-Uniform Physical Structure Model for Understanding the Electrochromic Behavior of Tungsten Oxide Thin Films' and R.A. Roy (1985) 'Evolution of Morphology in Amorphous and Crystalline Silicon Carbide Sputtered Films'] have provided a base of data on the evolutionary growth development of thin film morphology so that realistic computer simulations of the cross-section evolution could be attempted. Several typical evolution simulations are given in Figure 1. The model at present is purely geometrical and contains no physics per se. The shapes we generate, however, correspond to experimental data and by correlating the geometrical parameters with deposition parameter/processes, we expect to develop a useful geometrical model which can potentially predict evolutionary growth behavior.

The cross-sectional, 2-dimensional geometrical model, as typified in Fig. 1, has been used to study the effects of random seeding density, the growth

cone angle, the amount and method for cone deflection toward the incident vapor direction, and comparative surface roughness. These results are being compared to results from large scale random ballistic aggregation computer simulations onto surfaces which are being done by, and in collaboration with, Paul Meakin (Dupont, Wilmington, DE) and Len Sander (University of Michigan, Ann Arbor, MI). The visual similarity between the morphology developed by the geometrical model, the computer aggregation model, and experimental data is very encouraging and quantitative correlations are underway.

If, as we have suggested, thin film property variations (usually orders of magnitude) are controlled primarily by these low density void regions that define the internal morphological boundaries, it will be important to mathematically describe them. Properties such as electromigration, diffusion, post-deposition oxidation, film stress, and optical scattering are expected to vary as the size, shape, and distribution of the void network changes. One attempt to model this system is to consider the geometrical Sierpinski gasket, develop ways of generating a quasi-random gasket, and to consider the diffusion, scattering, etc. from these gaskets and related boundaries that they define. Work is progressing in this general area. As a first attempt in this direction we have explored a new class of planar fractals termed Pascal-Sierpinski Gaskets (see attached paper).

PAPERS PUBLISHED

Russell Messier and Joseph E. Yehoda, 'The Geometry of Thin Film Morphology,' J. Appl. Phys. (in press).

Neal S. Holter, Akhlesh Lakhtakia, Vijay K. Varadan, Vasundara V. Varadan and Russell Messier, 'On a New Class of Planar Fractals: The Pascal-Sierpinski Gaskets,' J. Phys. A (in press).

PAPERS PRESENTED

Russell Messier, 'Morphology of Surface deposits,' Symposium on Multiple Scattering of Waves in Random Media and Random Rough Surfaces, July 29 - August 2, 1985, University Park, PA.

Invited Seminars and Colloquia were presented throughout the year on the topic of thin film morphology at various institutions (Naval Postgraduate School in Monterey, CA; Westinghouse in Pittsburgh; Naval Weapons Center in China Lake, CA; OCLI in Santa Rosa, CA).

THESIS

Ammar Kouki, Bachelor of Engineering Science (May, 1985), 'Can the Morphology of Thin Films Grown by CVD Be Explained Using Fractal Theory?'

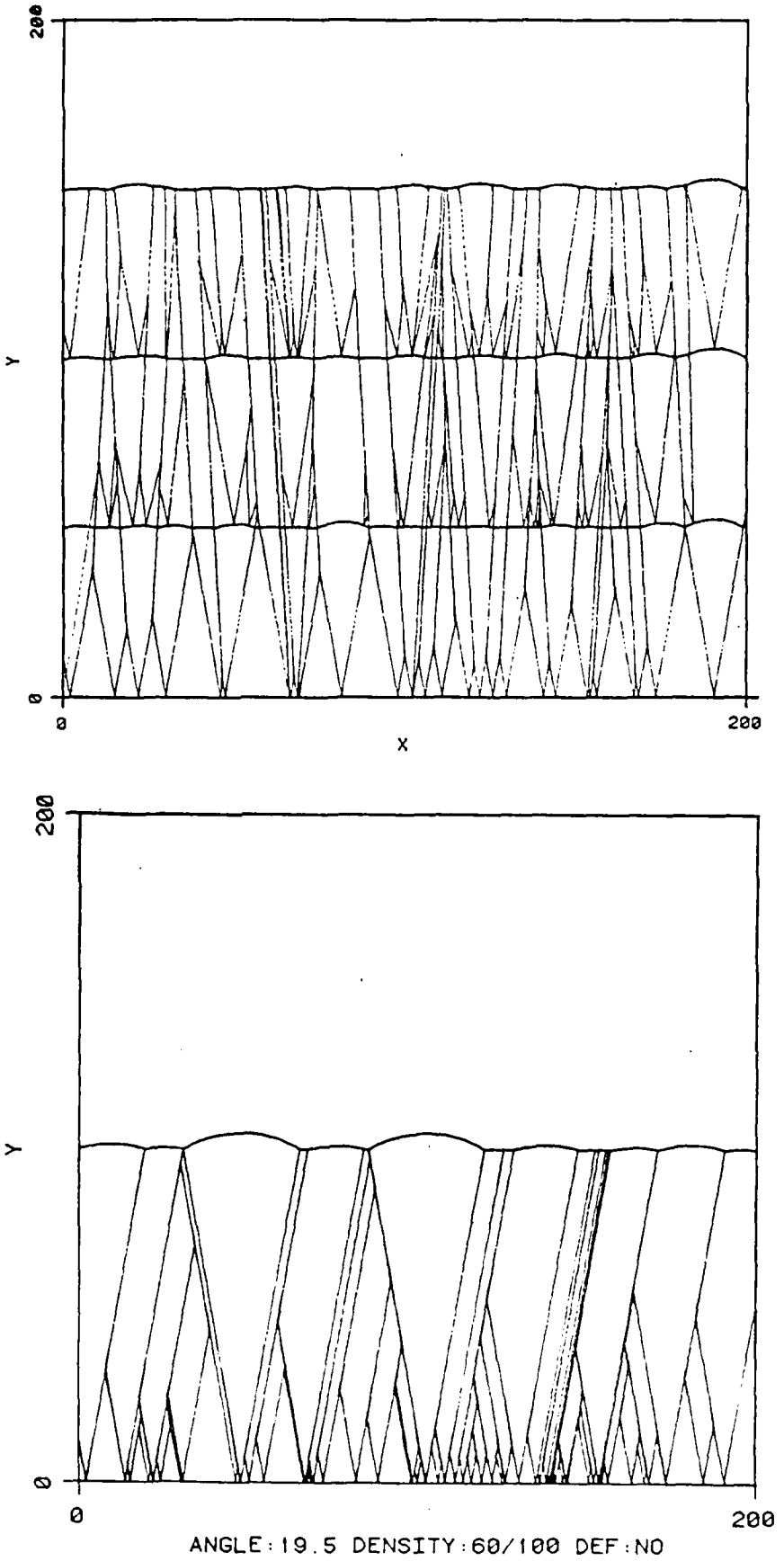

Fig. 1. Typical geometrical morphological constructions. The units are relative but, for example, could be in nanometers, thus representing the morphological development of a 150nm thick film.

THE GEOMETRY OF THIN FILM MORPHOLOGY

Russell Messier and Joseph E. Yehoda
The Pennsylvania State University
Materials Research Laboratory
University Park, PA 16802

ABSTRACT

The columnar morphologies commonly found in all vapor-deposited thin films prepared under low mobility conditions have been classified by several variations of what have been termed structure zone models. Such morphological structures are found to have a strong similarity in shape and form over six orders of magnitude in film thickness and three orders of magnitude in magnification for films of a given thickness. Thick (45mm) pyrolytic graphite films are shown to be a good demonstration of the continuous growth evolution of conical shaped units. Due to competition for growth each cone eventually goes through a death stage. A model based upon these general structural observations is presented and is shown to be a geometric construction similar to a Sierpinski gasket. The origin of this morphology seems to be the natural clustering which occurs due to the random process of ballistic aggregation.

J. Appl. Phys. (in press)

INTRODUCTION

Over the last 15 years there have been three distinct steps taken in the classification of thin film morphology[1-3]. Movchan and Demchishin[1] were the first to observe that regardless of the thin film material, its morphological structure is what is universally related to a normalized, or reduced, temperature T/T_m where T is the actual film temperature during deposition and T_m is its melting point, both in K. They defined three rather distinct structure zones.

Whereas Movchan and Demchishin[1] prepared their films by e-beam evaporation, Thornton[2] used magnetron sputtering and showed that both T/T_m and a second parameter, sputtering gas pressure, have a significant and classifiable effect on thin film morphology. Although neither well understood nor even clearly recognized, the reduction in film morphology size and resulting film densification with decreasing gas pressure is probably related to some type of ion-bombardment phenomenon such as elastically backscattered sputtering gas atoms.[4] This apparent bombardment effect, not present in evaporation methods, led Thornton to introduce a fourth transition zone, between Zones 1 and 2, called Zone T in which the films are much denser and have a smoother surface morphology than the two surrounding zones.

In a related set of papers[5-8] on thin films prepared by rf-sputtering, in which the sputtering plasma is in contact with the substrate, the plasma induced self-bias potential has been shown to be directly related to this reduction in morphology (i.e., emergence of Zone T). Somewhat surprisingly, rf-sputtered film morphologies could be classified quite well with Thornton's structure zone model (SZM) which was developed for magnetron sputtered films. Recently an extension to this work, in which a general morphological evolution with increasing film thickness has been recognized,[8-10] has resulted in a 3-parameter evolutionary SZM[3] which describes more precisely the preparation processes -- physical structure relations in the low mobility range ($T/T_m \lesssim 0.5$) of preparation conditions. With increasing bombardment and/or temperature, the rate of evolution of dominant morphology (ie., average size of morphological features viewed at the lowest possible magnification) decreases. For conditions of low T/T_m and bombardment this dominant surface morphology size is nearly linear with the ~ 3/4 power of the film thickness.[8]

The smallest size structural unit observed in the films prepared at low mobility conditions is an ~10-30Å size cluster which is most clearly viewed by field ion microscopy.[3,8-11] However, because this is near the resolution limit of conventional transmission electron microscopy (TEM), it has generally been the ~100Å size physical structure networks, observed in an underfocused or overfocused phase contrast TEM mode,[12] which have been easiest to recognize. Thus there is considerable literature recording the ~100Å sized honeycomb-like void networks for a broad range of thin films including Pt,[12] CdO,[13] permalloy,[13] Fe-B,[14] NbN [15] Si_3N_4,[16] (V,Ti)C,[17] Gd-Co,[14,18] Al,[19] TaN,[20] C,[21] Ge,[11,21-23] Si,[24] and Si:H.[10,25] This list includes metals, semiconductors, and insulators and both amorphous and crystalline films in each category. Furthermore, this structure is not unique to the deposition technique but has been found in all vapor-deposited films as well as electrodeposited films. The only common link between all these structurally anisotropic materials is that they were prepared under conditions of low mobility.

This similar 'size-shape' observation leads one to consider a common mechanism for the origin of anisotropic morphology at low adatom mobilty. The main approaches which have been taken involve atomic shadowing,[14,26-28] selective diffusion and nucleation,[22] coalesence- induced void formation,[12,21,29] stability of surface irregularities,[30] and energy minimization of topology.[31] All of these studies are at best semiquantitative which is in large part due to the random nature of the honeycomb-like morphological structures. Furthermore, there have been no studies to-date even attempting to quantify this structure.

Without doing any new experiments but just considering past experience and several relatively new areas of study - fractal geometry[32] and ballistic aggregation[33] - another approach to modeling the origin and evolution of anisotropic morphology can be suggested. As will be shown this model considers the random atom-by-atom aggregation process of film growth, is consistent with a wide range of observations,and has the potential for being quantitative. In this paper we will present some new results showing that thin film morphology is generally cone-shaped (i.e., structure evolution is <u>continuous</u>), that there is a competition for growth (i.e., all growth cones will eventually die), and that this general process occurs at all levels of morphology development from initial aggregation clusters (~10-30Å) all the way

to surface structural features with cm-size dimensions.

RESULTS

The similarity in shape of the morphology of films at different evolutionary growth stages has been suggested recently.[3,8-10] Figures 1(a)-(e) rather clearly, though qualitatively, shows this similarity in the morphology of various thin films which cover a range of thicknesses, from 10^2 to 10^8Å. These micrographs are representative of a wide range of thin film materials as seen in our recent studies and previous literature. It is also noted that very thick films (~1cm), Figure 1(e), such as those obtained on the walls and fixtures of production deposition chambers, show a similar structure with the additional feature of large surface relief. This often gives such films a mountainous appearance which coincidentally is similar to the fractal mountains generated by computer simulations.[32] One should also note the similarity between the different thin film physical structures, and the surface structure of cauliflower, Figure 1(f), which is formed by a competition between randomly branching structures. Thin film morphologies have been called 'cauliflower-like' for many years and, as will be discussed later, this analogy is probably not fortuitous but results from similar physical principals. Also, in the area of geomorphology there are a whole host of naturally occurring minerals and rocks (eg. hematite, malachite smithsonite, agates) which show this similar surface morphology, and are referred to as botryoidal and reuniform mass structures.

Pyrolytic graphite films are prepared by the thermal decomposition of methane at a substrate temperature of 1700-1900°C ($T/T_m \approx 0.5$), and thus fit the criteria for columnar structure development at the upper end of Zone 1/Zone T in the SZM classification schemes. The morphology of pyrolytic graphite films, as seen in Figure 1(d) provides an important example. First, despite the fact that the graphite structure and related carbon bonding is highly anisotropic and the film is highly crystalline, the morphology is essentially the same in shape as much thinner isotropic, amorphous films. Second, since pyrolytic graphite is easily cleaved, it is possible to look at the development of the physical structure at ~1mm increments in a 45mm thick sample.[34] Thus it allows for an absolute comparison of the evolution of the

morphological structure.

In Figure 2 are presented just six micrographs in order to demonstrate this evolution of morphology. The whole series of micrographs definitely shows that the structural features evolve continuously and that this evolution appears to result from a continual competition of smaller morphological units [most clearly seen as the substructure in Figure 2(a) and 1(d)]. In the sequence one can follow the growth of individual features (eg. see the box in Fig. 2a) and note that the largest features in the final morphology (Fig. 2f) evolved in general from the dominant features in the earliest stages of growth shown (Fig. 2a). This is not meant to imply that the largest features always win in their growth competition during film evolution but rather that they have a greater probability to continue their growth in size.

In Figure 2f, it can also be seen that the substructure within the largest (dominant) morphological features is similar to the smaller sized morphology seen in Figure 2a. This concept of larger morphological structure having continually smaller and smaller structure is shown in Figure 3, where, for a single film thickness, the morphology is explored over nearly three orders of magnitude in magnification. Again the general form of the morphology seems to remain nearly the same. It is also interesting to follow the approximately circular feature in Figure 3b (located near the center of the rectangle) and notice that the perimeter becomes more convoluted as the magnification is increased. More detailed results of this study will be given in another paper.

The cross-sectional view of the pyrolytic graphite [Figure 4(a)] and e-beam evaporated film [Figure 4(b)], shows both the continuous nature and inherent competition in the evolution of the physical structure. The larger columns are seen to be parabolic-like in profile with an internal structure consisting of smaller columns. Similar, quantitative results have been obtained recently for SiC films.[8] Such growth features were first recognized in pyrolytic graphite 20 years ago.[35] Two types of nucleation and growth processes have been recognized, singly nucleated and regeneratively or continuously nucleated. In the context of the previous discussion and observations, the difference between singly and continuously nucleated pyrolytic graphite is primarily in terms of the aspect ratio (height-to-width) of the columns. For singly nucleated films the aspect ratio is much higher and all the columns appear to originate at the substrate-film interfaces

whereas in the continuously nucleated case, new nucleating centers are constantly being formed throughout the thickness of the film.

A final observation is that some of these columns will dominate while others will recede. This can be ascribed to a simple geometric competition between adjacent columns, where the larger ones represent the former while the smaller represent the latter. A simple computer model shows this in Figure 5, while Figure 4 shows this directly in cross-section. This geometric competition can also be inferred, indirectly, from the series of micrographs (Figs. 2 and 3) showing the evolution of surface morphology. Similar observation in both our work and others have also shown this same growth-death competition. However, there has been no discussion to-date as to its significance. In this context it is noted that the previous description of nodular growths, [40] as emenating from multiply nucleated sites followed by growth competition, may not be an exception, but rather just an extension to the general rule. In all cases so far this direct observation has been for very thick films in which case microscopic resolution and sample preparation have not been a problem. The only indirect observation of this parabolic-like conical growth is provided by our previous observations of the dominant physical structure size as a function of film thickness.[3,8-10]

DISCUSSION

In the foregoing discussion it has been shown that the dominant physical structure of thin films appears self-similar. Obviously more quantitative data describing the shape and form of these structures as well, as their detailed internal structure, will be required. In the following discussion we will briefly describe the general form of the physical structure and evolution of vapor-deposited thin films prepared under low adatom mobility conditions as gleaned from this and related studies. An attempt will then be made to suggest future critical experiments to test this model as well as address the possible origin of this self-similar morphology behaviour.

The Sierpinski gasket[32] is an easily understood geometrical construction since it is symmetrical. It is a symmetric array of common shaped diamonds of varying size in which the larger diamonds are built from an ordered array of smaller diamonds. This object fills two dimensional space and can be envisioned as a three-dimensional space filling object composed of

inverted right circular cones. The important point of this construction is that it can be extended to both larger and smaller sizes by continuing the evident repetitive pattern generation process. It is also a fractal construct.[32]

The proposed model for the general morphology of a thin film prepared under low adatom mobility conditions is given in Figure 5. The vertical axis is film thickness with relative dimensions on a log-scale. The exact slopes of the sides of the growth-death cones may not always be linear, as displayed on this log-linear plot, but may vary under different preparation conditions. For instance, when bombardment effects are dominant the evolution of the morphology becomes much slower,[3,43] which would result in a smaller growth angle for the conical-like columns. The initial nucleation sites are randomly distributed and the evolution is depicted for only those sites which dominate within the evolution distance shown. Each of the gaps within the early stages of this structure can easily be filled by a similar construction as that shown and is only limited by the ability to draw them. Likewise, this structure can be extended to thicker films.

This model implies a common origin and evolution. Furthermore, whatever the nature of the origin is, it must be repeated over and over throughout the evolution of the structure. A critical question, then, is what is the size and shape of the original 'building block' for this thin film construction, and can one use the concept of fractal geometry to describe the apparent self-similarity in the thin film physical structures. A partial answer to this question has been offered by computer simulations of the random aggregation of hard discs on a surface.[14,26-28] This atomic self-shadowing mechanism shows that structural anisotropy, with dimensions on the order of 10Å, is a natural occurrence of such an atom-by- atom process. This mechanism appears to account for changes in orientation of film structure with changes in incident angle of the arriving vapor species according to a tangent rule.[14] Furthermore, direct observation of thin film structure by field ion microscopy appears to confirm this concept of clustered, columnar structures.[11]

More extensive computer simulations on the random ballistic aggregation of particles now show that these correlated density fluctuations do exist.[33] However, recent results on large systems of particles (eg. 10^8particles simulating a film ~600Å thick) now show that the overall resulting anisotropic

structure is not a fractal and does not strictly follow the tangent rule.[41] In a way this is an expected result since a fractal object will approach zero density if made large enough. This is clearly not the case in real films such as the graphite example.

The answer to this dilemma of a non-fractal origin to a fractal looking object may rest in considering what it is in thin film growth that makes it appear self-similar. It is, in fact, the dominant morphological structure in a two dimensional projection which shows the quality of self-similarity. And it is these dominant features, surrounded by regions of lower density and commonly called voids, which are shown in Figure 5. These larger void networks appear to result from a competition for growth of smaller void networks, the smallest ones surrounding clusters which apparently are non-fractal. Beyond these general statements there may very well be some specific geometrical construction principles that could explain the general observed behavior, such as parabolic-like growth- death cones, which remain to be understood. One interesting approach is to consider the branching structure in the growth of cauliflower, Figure 1(f), the structure of which appears similar to that of the thin films in Figures 1 and 2. Other approaches based upon surface irregularity initiation, such as constructing contour lines of constant depth,[33] may also be fruitful especially when combined with columnar, competitive growth cones which are definitely present.

If this model is generally correct, then the distribution function of columnar sizes in the thinner films (~100Å) will be very important in predicting the eventual evolutionary growth morphology. The basic assumption made both here and in generating Figure 5 is that the larger columns (i.e., tail of the distribution function) are distributed randomly and have a proportionately higher probability of growing larger before entering their death stage. As the larger morphological units enter this later stage they are no longer the largest cone-like units with respect to their immediate neighbors and their relative probability for growth decreases. As each dominant growth cone gets larger they will always eventually come into contact with ones which are even larger.

The primary effect of bombardment, in this context, may turn out to be one of redistribution of adatoms from the larger cones to the smaller ones, thus drastically altering the distribution function. Such local redistribution would be expected to be greatest at the edges of the growth

cones where the fewest bonds per atom are present and downward sputtering is possible. This would be seen as a much sharper distribution function of initial column sizes with a much smaller growth angle. Molecular dynamic sputtering simulations at low energies on thin 'crystals' show this to be a probable event[42] and recent experiments[43] on SiC sputtered films lend further support.

CONCLUSION

The physical structure of films prepared under low mobility conditions are generally recognized as columns, separated by void regions, connected in a rather chaotic, ill-defined, honeycomb-like structure. Until recently there has been little recognition that these structures evolve with film thickness. In this paper we have brought together a number of past observations, presented several new results on continuous physical structure evolution in pyrolytic graphite, and proposed a general structural evolution model which is based on the self-similar nature of the dominant void network structures. This model is intended as a first attempt at refining our current knowledge and is expected to be revised as more quantitative data, such as suggested in this paper, becomes available.

ACKNOWLEDGEMENTS

The contribution of Paul Meakin (at E.I. DuPont de Neumours) to the inspiration of this random fractal-like structure model, as well as extensive computer calculations on the early stages of thin film growth showing its non-fractal nature, are gratefully acknowledged. This work was supported by the Air Force Office of Scientific Research under Grant No. AFOSR-84-0149.

REFERENCES

1. B.A. Movchan and A.V. Demchishin, Phys. Met. Metallogr. 28, 83 (1969).

2. J.A. Thornton, Ann. Rev. Mat. Sci. 7, 239 (1977).

3. R. Messier, A.P. Giri and R.A. Roy, J. Vac. Sci. Technol. A2, 500 (1984).

4. D.W. Hoffman and J.A. Thornton, Thin Solid Films 45, 387 (1977).

5. R.C. Ross and R. Messier, J. Appl. Phys. 52, 5329 (1981).

6. R.C. Ross and R. Messier, AIP Conf. Proc. 73, 53 (1981).

7. R.C. Ross and R. Messier, J. Appl. Phys. 54, 5444 (1983)

8. R.A. Roy and R. Messier, J. Vac. Sci. Technol. A2, 312 (1984) and R.A. Roy and R. Messier, Mat. Res. Soc. Symp. Proc. 38, 363 (1985).

9. A.P. Giri and R. Messier, Mat. Res. Soc. Symp. Proc. 24, 221 (1984).

10. R. Messier and R.C. Ross, J. Appl. Phys. 53, 6220 (1982).

11. S.V. Krishnaswamy, R. Messier, Y.S. Ng, T.T. Tsong and S.B. McLane, J. Non-Cryst. Solids 35-36, 531 (1980).

12. S. Nakahara, Thin Solid Films 45, 421 (1977).

13. S. Nakahara, Thin Solid Films 64, 149 (1979).

14. H.J. Leamy and A.G. Dirks, J. Appl. Phys. 49, 3430 (1978).

15. W. Wagner, D. Ast and J.R. Gavaler, J. Appl. Pys. 45, 465 (1974).

16. C.J. Mogab, P.M. Petroff and T.T. Sheng, J. Electrochem. Soc. 122, 815 (1975).

17. B.E. Jacobson, R.F. Bunshah and R. Nimmagadda, Thin Solid Films 54, 107 (1978).

18. S.R. Herd, Phys. Stat. Solidi (a)44, 363 (1977).

19. R.V. D'Aiello and S.J. Freedman, J. Appl. Phys. 40, 2156 (1969).

20. Y. Murayama, J. Vac. Sci. Technol. 12, 818 (1975).

21. A. Staudinger and S. Nakahara, Thin Solid Films 45, 125 (1977).

22. A. Barna, P.B. Barna, G. Radnoczi, H. Sugawara and P. Thomas, Thin Solid Films 48, 163 (1978).

23. T.M. Donovan and K. Heineman, Phys. Rev. Lett. 27, 1794 (1971).

24. A. Barna, G. Radnoczi, L. Toth and P. Thomas, Phys. Stat. Solidi (a)41, 81 (1977).

25. J.J. Hauser, G.A. Pasteur and A. Staudinger, Phys. Rev. B24, 5844 (1981).

26. A.G. Dirks and H.J. Leamy, Thin Solid Films 47, 219 (1977).

27. D. Henderson, M.H. Brodsky and P. Chaudhari, Appl. Phys. Lett. 25, 641 (1974).

28. S. Kim, D.J. Henderson and P. Chandhari, Thin Solid Films 47, 155 (1977).

29. J.R. Lloyd and S. Nakahara, J. Vac. Sci. Technol. 14, 655 (1977).

30. N.J. Shevchik, J. Non-Cryst. Solids 12, 141 (1973).

31. J.C. Phillips, Physics Today Vol. 35 (Feb. 1982), p. 27.

32. B.B. Mandelbrot, The Fractal Geometry of Nature, W.H. Freeman and Co., New York (1983), p. 131.

33. P. Meakin, Phys. Rev. A27, 2616 (1983).

34. Sample was obtained from D. Cummings, Pfizer Inc., Easton, PA 19042.

35. L.F. Coffin, J. Am. Ceram. Soc. 47, 473 (1964).

36. P. Swab, S.V. Krishnaswamy and R. Messier, J. Vac. Sci. Technol. 17, 362 (1980).

37. A. Grill and P.R. Aron, Thin Solid Films 108, 173 (1983).

38. J.A. Thornton and D.P. Ferriss, Thin Solid Films 40, 365 (1977).

39. J.A. Thornton, Thin Solid Films 40, 335 (1977).

40. T. Spalvins and W.A. Brainard, J. Vac. Sci. Technol. 11, 1186 (1974).

41. P. Meakin, private communication.

42. D.E. Harrison, Rad. Eff. 70, 1 (1983).

43. R.A. Roy, Ph.D. Thesis. The Pennsylvania State University (1985).

FIGURE CAPTIONS

Figure 1. Micrographs showing the similarity in morphology for various materials at different magnifications. These six micrographs cover approximately six orders of magnitude in morphological size. (a) TEM micrograph of a-Ge; (b) SEM micrograph of a-Si on glass substrate; (c) SEM micrograph of a-Si on polycrystalline Al substrate; (d) optical micrograph of pyrolytic graphite; (e) optical micrograph of thick metal film, and (f) photomicrograph of cauliflower.

Figure 2. The evolution of a surface feature in pyrolytic graphite as a function of thickness. Micrographs (a) through (f) are ~1mm thick slices approximately 1mm, 6mm, 8mm, 10mm, 14mm, and 20mm from the bottom surface of the sample, respectively. Note in particular the evolution of the features enclosed in the box in (a).

Figure 3. SEM micrographs showing the self-similarity in the morphological features of pyrolytic graphite as a function of increasing magnification, covering approximately two and one-half orders of magnitude. Each rectangle represents the area seen in the following micrograph. The bar markers represent: (a) 500μm; (b) 200μm; (c) 50μm; (d) 20μm; (e) 5μm; (f) 2μm.

Figure 4. (a) Cross-section of pyrolytic graphite showing conical-like growth-death cones. (b) Cross-section of thick e-beam evaporated film showing competition between conical-like structures.

Figure 5. A computer generated cross-section showing the growth-death competition of the proposed thin film morphology model. The cluster positions as well as the growth angles are distributed randomly.

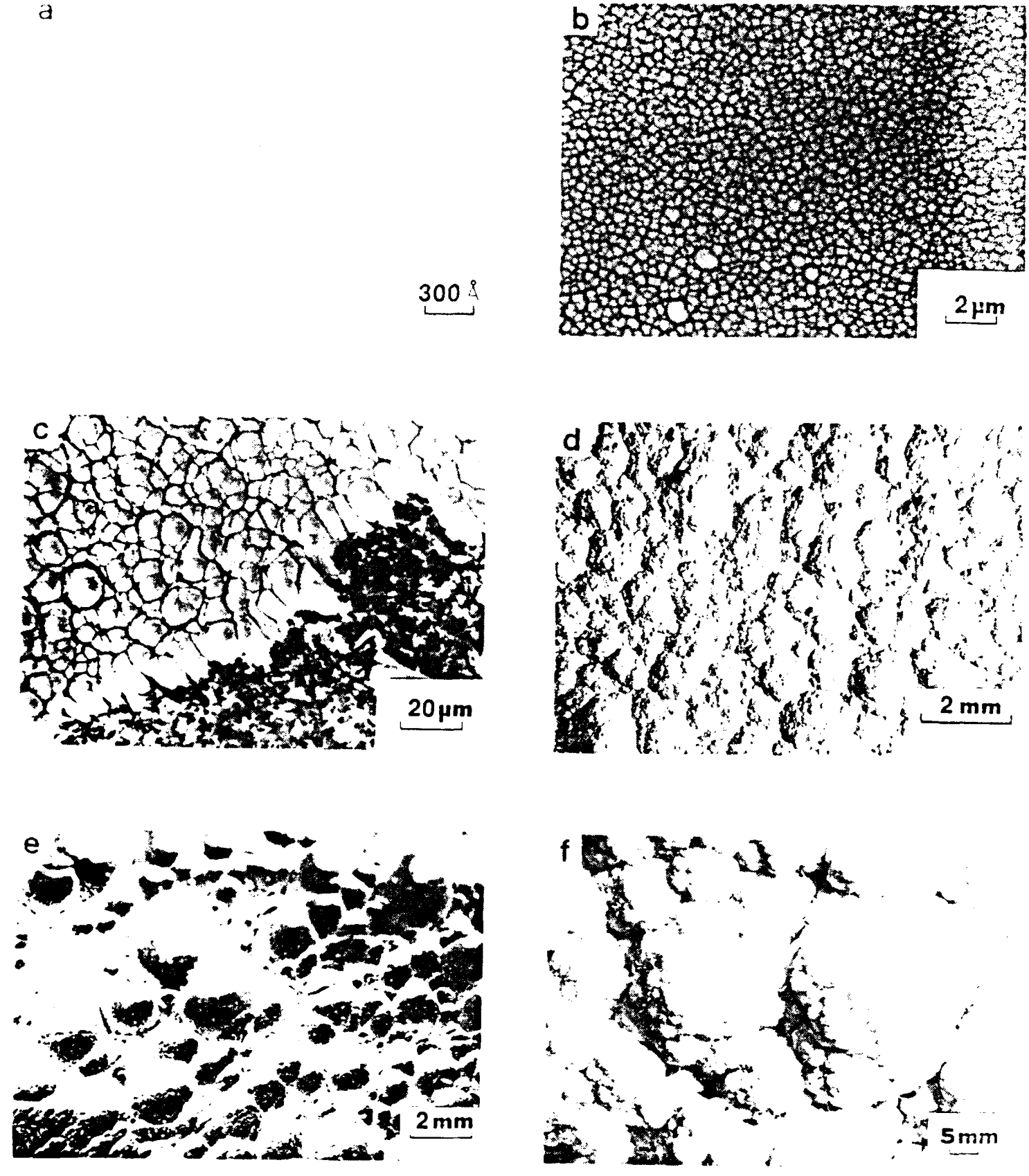
a
300 Å
b
2 µm
c
20 µm
d
2 mm
e
2 mm
f
5 mm

Figure 2.

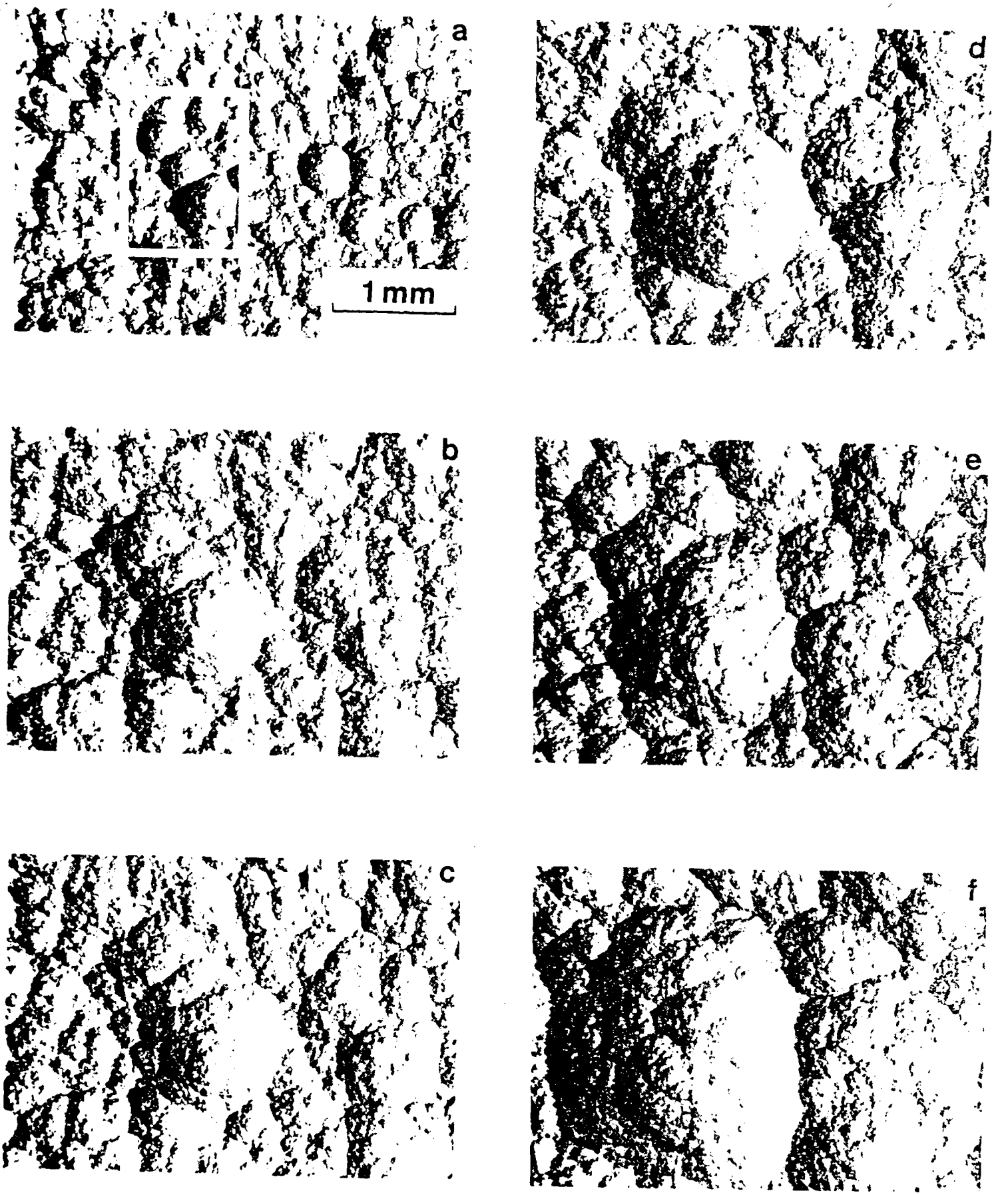

Figure 3.

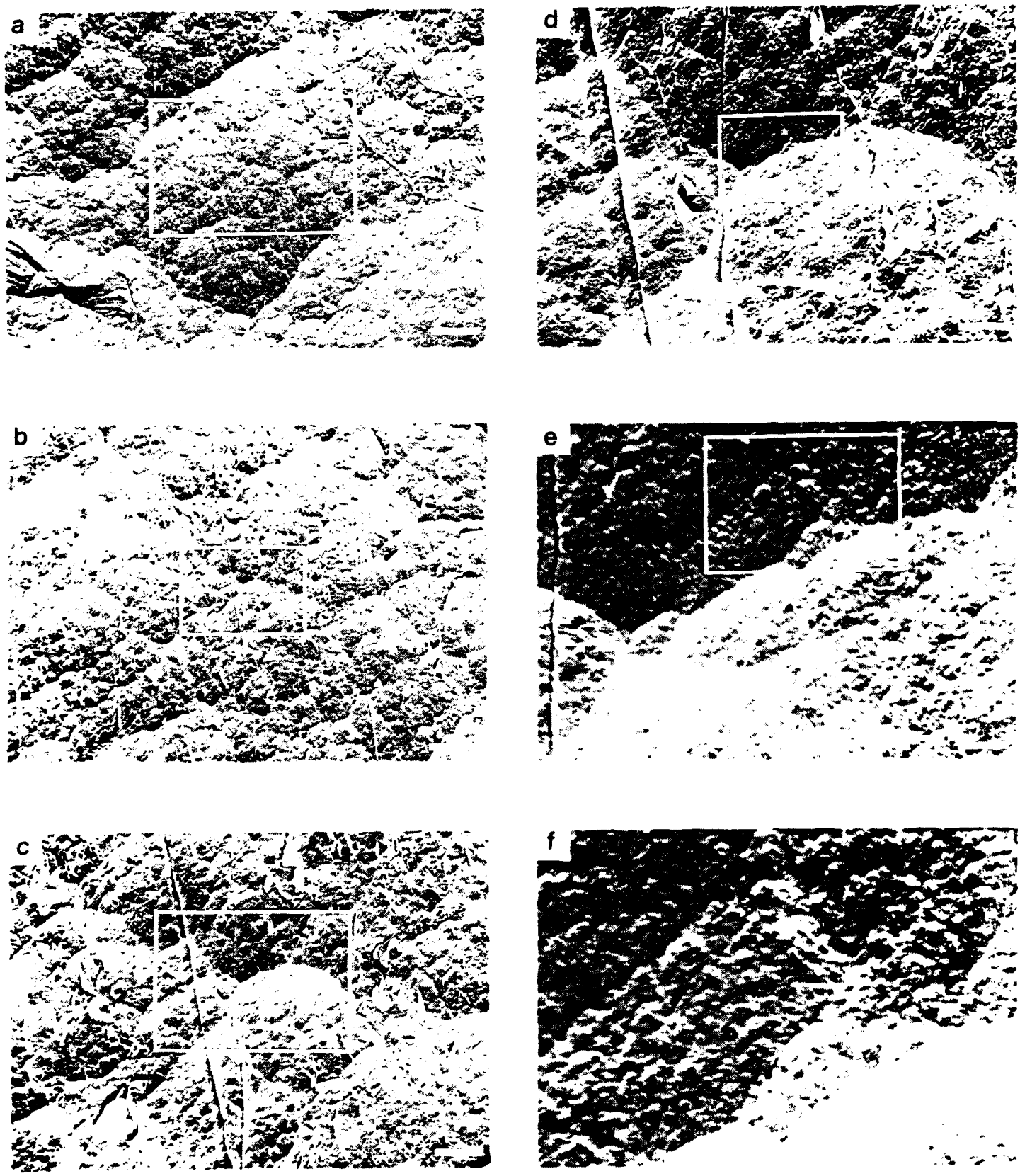

Figure 4.

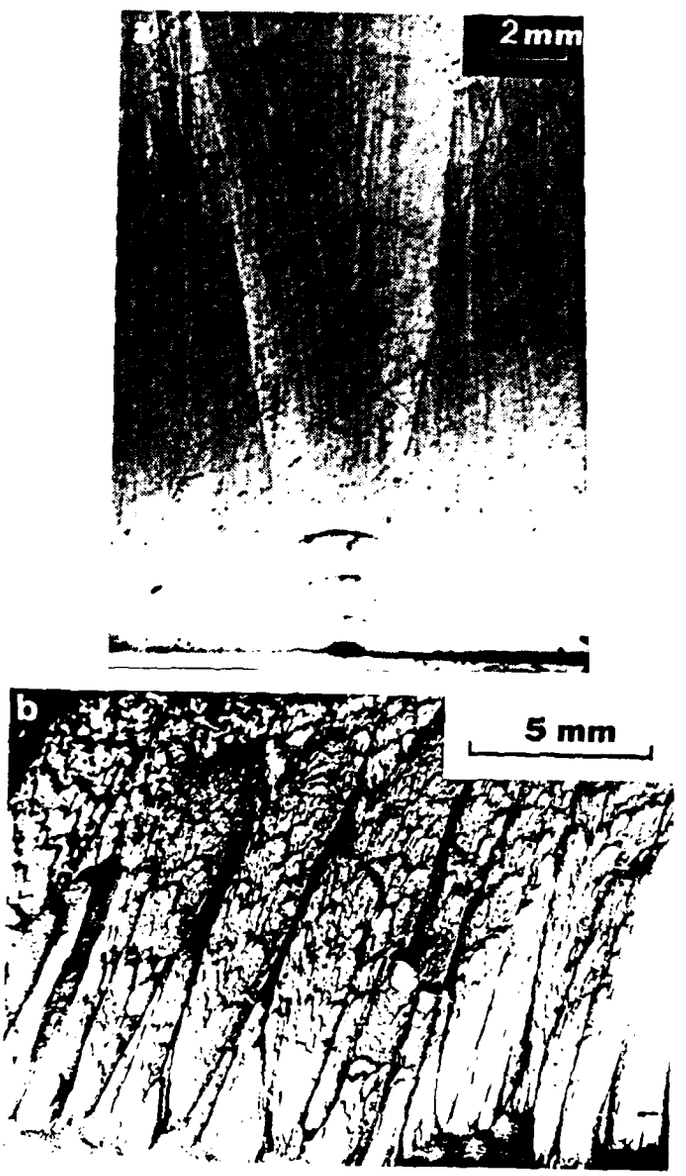

Figure 5.

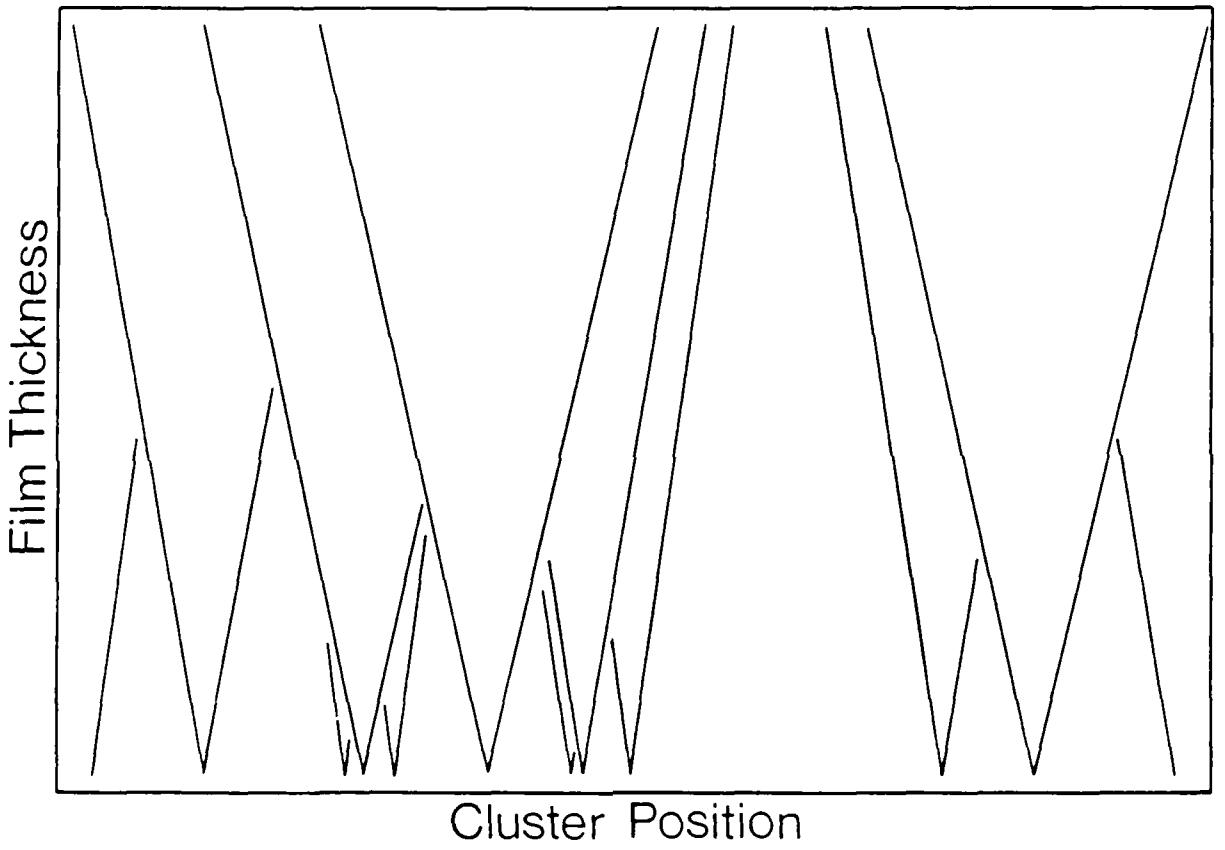

ON A NEW CLASS OF PLANAR FRACTALS : THE PASCAL-SIERPINSKI GASKETS

Neal S. Holter, Akhlesh Lakhtakia, Vijay K. Varadan and Vasundara V. Varadan
Laboratory for Electromagnetic and Acoustic Research,
Department of Engineering Science & Mechanics,
The Pennsylvania State University,
University Park, PA 16802 (USA).

and

Russell Messier
Material Research Laboratory and *the Department of Engineering Science & Mechanics,*
The Pennsylvania State University,
University Park, PA 16802 (USA).

ABSTRACT

A new class of planar fractals called the Pascal-Sierpinski gaskets is described, of which the well-known Sierpinski gasket is a special case. Some of these gaskets are true Mandelbrot fractals possessing non-integral dimensions as well as self-similarity; the remaining ones are not self-similar, but appear to have non-integral dimensions.

J. Phys. A (in press).

1. INTRODUCTION

Physics, in general, till recently has been greatly limited in its scope by the use of Euclidean geometry whereby all bodies possess integral dimensionality ranging from 0 to 3. But, to quote from the cover flap of Mandelbrot's celebrated work [1983], 'all clouds are not spheres, mountains are not cones, and lightning does not travel in a straight line.' The forms exhibited by nature differ so much from Euclidean objects that an entirely new geometry has had to be applied, principally by Mandelbrot himself [1983] but also by several others [e.g., Lovejoy 1982; Berry 1982; Walker and Jakeman 1982; Yehoda and Messier 1985]. The relatively huge amount of effort put forth in the last few years has resulted in the identification of several natural shapes as what are known now as *fractals*.

Fractals are bodies characterised by several properties. Among the more notable ones are their possession of non-integral or fractional dimensionality, and, self-similarity. Natural fractals are found to be scale-invariant over several length scales [Yehoda and Messier 1985]; whereas strictly geometric fractals are scale-invariant over all possible appropriate scales. An adequate discussion of these and other properties of fractals can be found elsewhere [Mandelbrot 1983], for which reason, they will not be reviewed in any detail here.

Though natural fractals occur in any landscape and in such 'random' structures like thin films, and are, as a result, probably more familiar, strictly geometric fractals are not of solely academic interest. The Sierpinski gasket (fractal dimension = log3/log2), on which a great deal of attention has been devoted by Mandelbrot [1983], is a geometric fractal of interest in percolation morphology studies. In studying percolation through lattices, it was observed by Gefen *et al* [1980; 1981] that the branching structure of the Sierpinski gasket (and of its 3- and 4- dimensional analogues) proves to be a promising model of the structure of the cluster backbones. Recent work on the Sierpinski gasket has also been reported by Stephen [1981], Rammal and Toulouse [1982] as well as by Alexander and Orbach [1982].

In this communication, the authors are primarily concerned about describing a new class of geometric fractals derivable from the well-known Pascal's triangle, and of which the Sierpinski gasket is a special case. It will be shown here that with the complete (i.e., infinitely large) Pascal's triangle as a base, fractal surfaces ranging upto a dimension of 2.0 can be constructed; the unaltered Pascal's triangle being of exactly 2.0

dimensionality. Several other structures also emerge which do not possess self-similarity in a strict sense, but which appear to have non-integral dimensionality.

2. THE PASCAL-SIERPINSKI GASKETS

Pascal's triangle constitutes an equiangular triangular grid whose rows shall be labelled by $n = 1,2,3,...$, each row containing n nodes $\{n, p_n\}$, $p_n = 1,2,3,...,n$. Attached to each of the nodes on this triangular grid is a number ${}^{n}C_{p_n} = n! / [(n-p_n)!\, p_n!]$, which are nothing but the p_n-th coefficients of the binomial expansion of $(x + y)^n$. As is readily seen, the triangular grid thus formed is infinitely large, the numbers ${}^{n}C_{p_n}$ growing without bounds as n increases. Incidentally, ${}^{n}C_1 = {}^{n}C_n = 1$. An extensive table of these numbers can be found in a handbook by Abramowitz and Stegun [1970].

The fractals to be described here can be evolved from any truncated Pascal's triangle of a suitably large size; and they shall be referred to as the Pascal-Sierpinski gaskets hereafter. The algorithm for generating them now follows.

First of all, a label ${}^{n}L_{p_n}$ is attached to each of the nodes $\{n,p_n\}$. Any integer $N > 1$ may now be chosen, and the labels ${}^{n}L_{p_n}$ are defined by

$${}^{n}L_{p_n} = 1, \quad \text{if } {}^{n}C_{p_n} \text{ is } \textit{not exactly divisible} \text{ by N} \tag{1a}$$

and

$${}^{n}L_{p_n} = 0, \quad \text{if } {}^{n}C_{p_n} \text{ is } \textit{exactly divisible} \text{ by N.} \tag{1b}$$

The resulting map of the labels ${}^{n}L_{p_n}$ superimposed on the triangular grid constitutes a Pascal-Sierpinski gasket of order N. It will be now shown that the gaskets thus formed may be considered as fractals.

3. THE FRACTAL DIMENSION

Let each of the nodes in this map be treated as having a mass ${}^{n}L_{p_n}$. The grid will contain several voids and several filled areas, and Figs. 1 - 5 show the generated gaskets when $1 \leq n \leq 64$, while N varies from 2 to 6.

Inspection of these gaskets shows that when N is a prime number, they are self-similar in the Mandelbrot sense. Their fractal (similarity) dimension d_N can then be easily computed to be

$$d_N = \log \{ N(N+1)/2 \} / \log \{N\}, \qquad (N \text{ prime}) \tag{2}$$

which turns out to be 1.5849625 for N = 2, and

$$\mathrm{Lim}_{N \to \infty} \{d_N\} = 2, \qquad (N \text{ prime}). \tag{3}$$

Furthermore, for N = 2, the gasket generated is nothing but the Sierpinski gasket [Mandelbrot 1983].

Next come the cases when N is an integral power of a prime number. In such cases, as in Fig. 3 for N = 4 = 2^2, visual inspection alone suffices to show that the resulting gaskets are self-similar. However, a simple formula like (2) for the fractal dimension d_N could not be deduced by the authors for these cases.

Finally, come the cases for all other values of N > 1, when N is neither a prime nor an integral power of a prime, as in Fig. 6 for N = 6 = 2×3. Visual inspection extended upto n = 198 rows did not show any self-similarity in these gaskets. However, if the factorisation

$$N = \prod_i (j_i)^{k_i} = \prod_i N_i \tag{4}$$

is made, where all k_i are real positive integers and all j_i are primes, then the gasket of order N can be synthesised from the gaskets of orders N_i by the operation

$$\textbf{gasket } \{N\} = \textbf{gasket } \{N_1\} \oplus \textbf{gasket } \{N_2\} \oplus \textbf{gasket } \{N_3\} \oplus ..... \tag{5}$$

where $\oplus$ denotes an OR operation [Baron and Piccirilli 1967]. The operation OR between any two gaskets of orders N_i and N_j is performed by overlaying one on top of the other such that their like-numbered nodes coincide exactly. Then for each node $\{n,p_n\}$ of the resulting overlay, the resulting label is given by

$${}^{n}L_{p_n} \{N_i \oplus N_j\} = {}^{n}L_{p_n} \{N_i\} \oplus {}^{n}L_{p_n} \{N_j\}, \tag{6a}$$

where the familiar rules of Boolean algebra

$$1 \oplus 1 = 1; \; 1 \oplus 0 = 1; \; 0 \oplus 1 = 1; \; 0 \oplus 0 = 0, \tag{6b}$$

apply. Because of (5) it is conjectured that this last class of the Pascal-Sierpinski gaskets should also possess fractal dimensions, though they are not self-similar.

4. NUMERICAL DETERMINATION OF FRACTAL DIMENSION

Since a fairly general method of determining the fractal dimension d_N was needed, in view of the fact that the formula (2) is applicable only for prime N, the mass-radius fractal dimension D_N was determined for the gaskets of Figs. 1 - 5. As has been mentioned earlier, each of the nodes in the gaskets was given a mass

${}^{n}L_{p_n}$, while the node {1,1} was treated as the datum point for measurement of the distance r. Since the triangular grid is equiangular and its rows equispaced, the nearest-neighbour distance between the nodes was taken to be unity. It may be noted that if these gaskets are not fractal, then $D_N = 2.0$ should result from such a procedure; if, however, they are, then D_N should converge to d_N, $1.0 < d_N \leq 2.0$, as their truncation levels are increased. Measurements were made by sweeping out 60°-wide, symmetric arcs of increasing radii r from the datum node, the sum of the labels ${}^{n}L_{p_n}$ covered in the sector giving the mass $m_N(r)$ of the sectoral plates thus formed. These computations were made for all gaskets of orders N = 2 - 5, with the number of rows set to be $n \leq 198$, 500 and 1000. Shown in Figs. 1 - 5, also are the plots of $\log_N \{m_N(r)\}$ versus $\log_N \{r\}$, for the gaskets truncated at n = 1000. Finally, through each of these plots a straight line was fitted, using a least-squares curve-fitting procedure [Worthing and Geffner 1948], for reasonably high values of $\log_N \{r\}$. The slope of this line is the mass-radius dimension D_N.

It is observed from Table I, where the computed D_N are given, that as the truncation level of the Pascal-Sierpinski gaskets is increased, the dimension D_N appears to be converging towards the 'expected' fractal dimension d_N for prime N. Likewise, even for the other cases of non-prime N, this data clearly suggests the existence of a fractal dimension.

Shown in Table II are the number of massless points for each of the 5 gaskets considered at levels of truncation n = 198, 500 and 1000. A comparison of Tables I and II reveals that $D_4 < D_5 < D_6$, even though the order 5 gasket contains more massless nodes than the gaskets of orders 4 or 6. Normally, one would expect that a larger number of massless nodes should give rise to a smaller D_N; yet, this is not the case here. And, although the gasket of order 6 is not self-similar, the other two are. This feature, that the larger number of voids is not related to a smaller mass-radius dimension, appears to be due to the differences in the textures of the pertinent gaskets [Mandelbrot 1983].

5. CONCLUSIONS

In summary, a class of gaskets named after Pascal and Sierpinski has been described here, of which the Sierpinski gasket [Mandelbrot 1983] is a special case. It is shown that the mass-radius dimensions of these gaskets are fractions are greater than unity but less than 2.0. Furthermore, some of these gaskets are self-similar

and, thus, form true Mandelbrot fractals. Conceivably, these gaskets are of use in modelling percolation clusters.

ACKNOWLEDGEMENT

This work was supported by the US Air Force Office of Scientific Research under Contract No. AFOSR-84-0149.

REFERENCES

Abramowitz M and Stegun IA 1970 *Handbook of Mathematical Functions* (New York : Dover).

Alexander S and Orbach S 1982 *Journal du Physique Letters* **45**, 625 {cited in Mandelbrot 1983}.

Baron RC and Piccirilli AT 1967 *Digital Logic and Computer Organization* (New York : McGraw-Hill).

Berry MV 1982 *J. Phys. A* **15**, 2735.

Gefen Y, Mandelbrot BB and Aharony A 1980 *Phys. Rev. Lett.* **45**, 855.

Gefen Y, Aharony A, Mandelbrot BB and Kirkpatrick S 1982 *Phys. Rev. Lett.* **47**, 1771.

Lovejoy S 1982 *Science* **216**, 185.

Mandelbrot BB 1983 *The Fractal Geometry of Nature* (New York : Freeman).

Rammal R and Toulouse G 1982 *Phys. Rev. Lett.* **49**, 1194.

Stephen MJ 1981 *Phys. Lett. A* **87**, 67.

Walker JG and Jakeman E 1982 *Opt. Acta* **29**, 313.

Worthing AG and Geffner J 1948 *Treatment of Experimental Data* (New York : Wiley).

Yehoda JE and Messier R 1985 *Appl. Surf. Sci.* **22/23**, 590.

TABLE I: MASS-RADIUS DIMENSION D_N

Order N	D_N			d_N
	$n \leq 198$	$n \leq 500$	$n \leq 1000$	
2	1.5681	1.5716	1.5738	1.58496
3	1.6134	1.6138	1.6218	1.63093
4	1.6567	1.6617	1.6688	-
5	1.6645	1.6688	1.6691	1.68261
6	1.6780	1.6712	1.6693	-

TABLE II : NUMBER OF MASSLESS NODES *versus* TOTAL NUMBER OF NODES

Order N	Number of Massless Nodes / Total Number of Nodes		
	$n \leq 198$	$n \leq 500$	$n \leq 1000$
2	15996/19701	107871/125250	448363/500500
3	14949/19701	101742/125250	437420/500500
4	12953/19701	091495/125250	393442/500500
5	13896/19701	091500/125250	409375/500500
6	12393/19701	088766/125250	395000/500500

FIGURE CAPTIONS

Fig.1 The Pascal-Sierpinski gasket of order N = 2. Shown are the first n = 64 rows of the gasket. The graph alongside plots the mass-radius variation for this gasket when the first n = 1000 rows have been considered.

Fig.2 As in Fig. 1 but N = 3.

Fig.3 As in Fig. 1 but N = 4.

Fig.4 As in Fig. 1 but N = 5.

Fig.5 As in Fig. 1 but N = 6.

Fig.1 The Pascal-Sierpinski gasket of order N = 2. Shown are the first n = 64 rows of the gasket. The graph alongside plots the mass-radius variation for this gasket when the first n = 1000 rows have been considered.

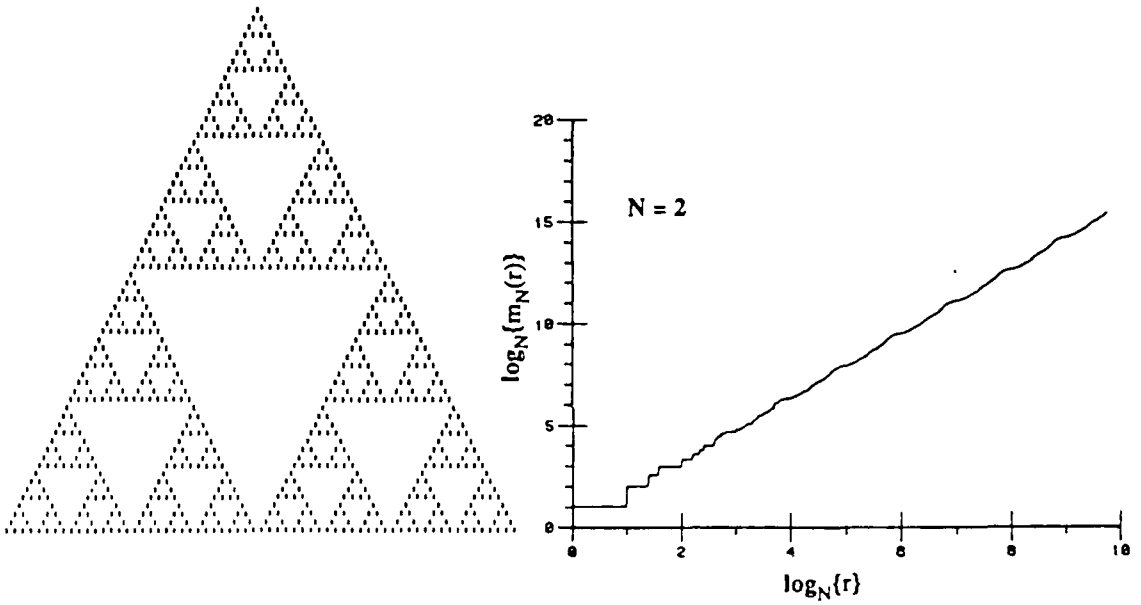

Fig.2 As in Fig. 1 but N = 3.

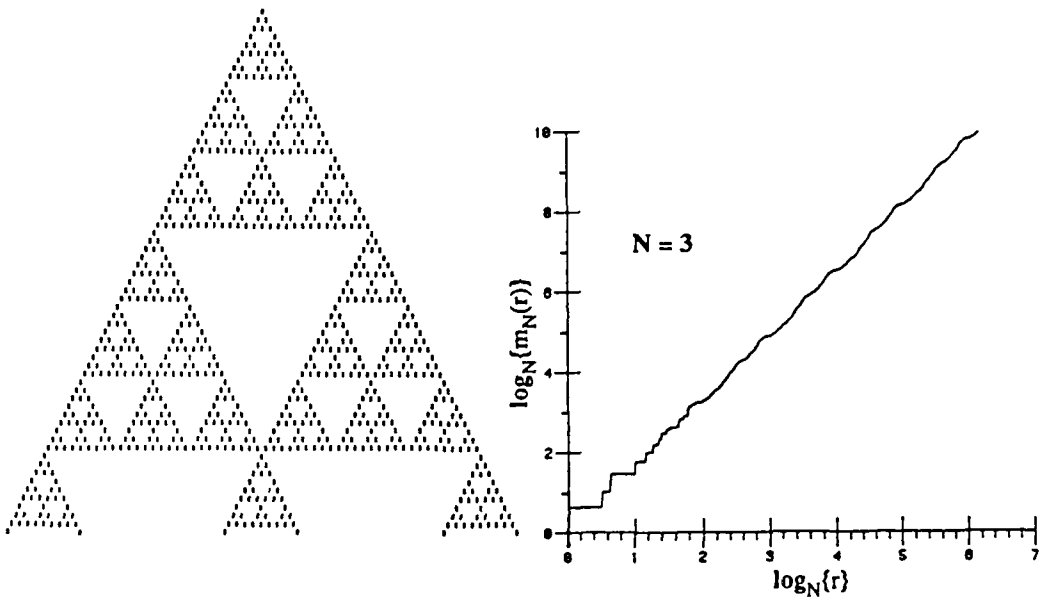

Fig.3 As in Fig. 1 but N = 4.

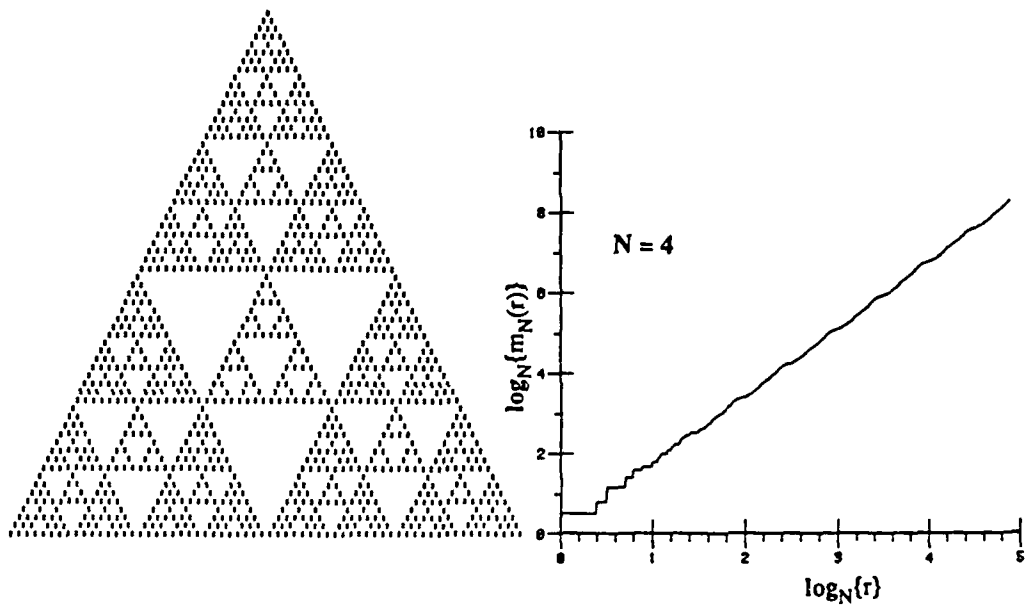

Fig.4 As in Fig. 1 but N = 5.

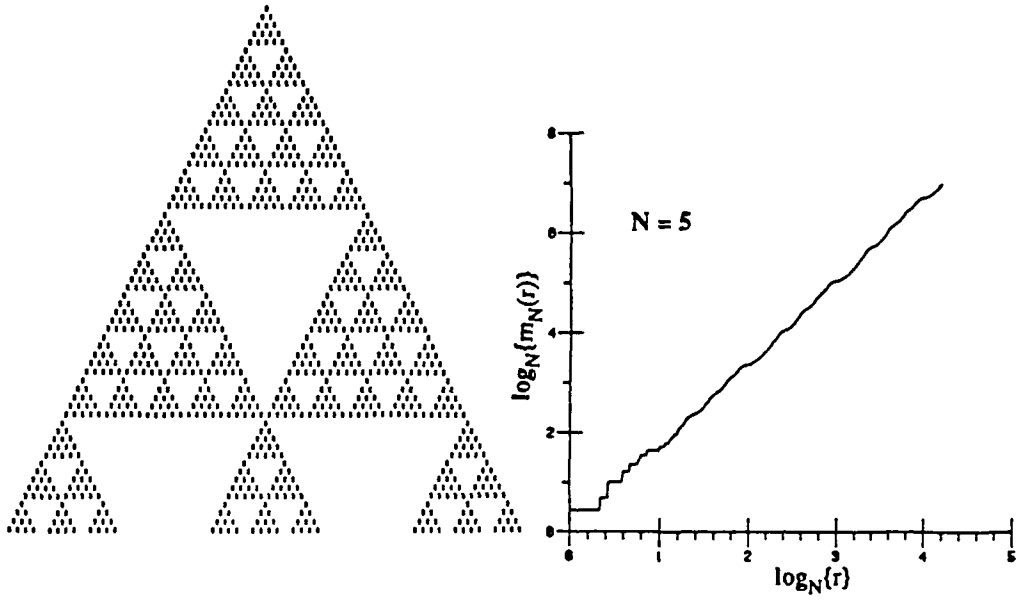

Fig.5 As in Fig. 1 but N = 6.

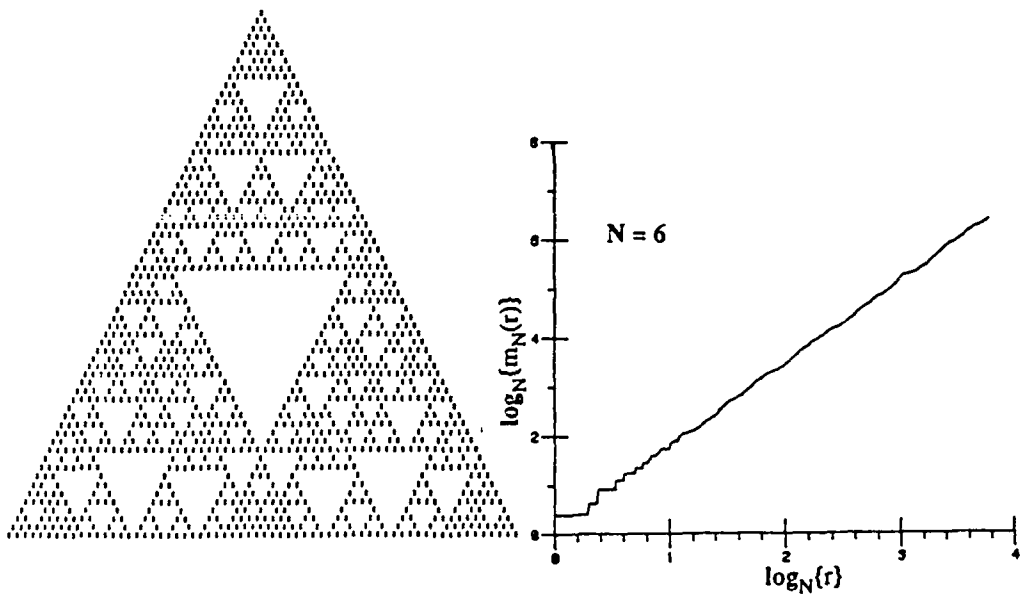

END

FILMED

1-86

DTIC